INFLUENCE OF PARAMETRIC VARIATION IN BANDGAPS FOR ONE-DIMENSIONAL STRUCTURES

Wanderson V. O. Monteiro[1], Cássio B. F. Gomes [1], Edilson D. Nóbrega[1]

[1]*Dept. of mechanical engineering,Federal University of Maranhão*
University City Dom Delgado,65085-580, São Luís,Maranhão, Brazil
wanderson.monteiro@discente.ufma.br, cassio.bruno@discente.ufma.br, edilson.dantas@ufma.br

Abstract. In engineering projects where the noise reduction or vibrations is desired, some control methodologies are applied in order to provide safe and comfortable environments. For that, structural dynamic analysis is done to verify the effects of wave propagation in the structure. Focusing on this analysis, a parametric variation on elastic rods phononic crystals (PCs) was performed. The rods are made by two types of materials spatially distributed periodically along its length. Each period will form a cell, in which was made the variation of the proportion of each material in order to observe its influence on the bandgap formation. Another approach to have the formation of the bandgap was the variation of the cross section of the cell. Those analyses were made both separately and assembled. It was used the Spectral Element Method – SEM to obtain the results. FEM was used to validate the results. Then, it was possible to obtain the rod behavior due the change of the proportion of materials and cross section. In the case of the two variations there was a coupling of Bragg scattering effect, allowing both an increase in its frequency band and in the attenuation level.

Keywords: Periodic structure, Phononic crystals, Wave propagation, Spectral Element Method, Bandgaps.

1 Introduction

In structural engineering projects, the control of vibration and noise levels is necessary. Furthermore, developing methods that predict and detect structural damage are essential factors to provide an environment that offers comfort and safety, Santos [1].

In the engineering field, Mead [2] was one of the pioneers in the study of wave propagation in periodic structures. His work showed that in an infinite beam with identical and equidistant supports, the harmonic motion with free vibration can be considered a group of sine waves. Which propagate in different directions and speeds.

Kushwaha [3] was one of the first authors to investigate the structure of phononic crystals (PC). Likewise, Sigalas, Economou [4], that through spheres inserted periodically in a homogeneous material, frequency gaps were verified. Therefore, phononic crystals can be defined as artificial materials that have unit cell periodicities with high impedance variation. The impedance difference is caused by the difference in properties between the materials that compose the cells, geometric discontinuities or boundary conditions, Hussein et al. [5].

One of the characteristics of PCs is the appearance, in the dynamic responses of the system, of regions where there is no wave propagation. These regions are known as bandgaps or Stop Bands, and the other frequency bands where there is wave propagation are called Passband. One of the ways to find the bandgaps is through the Spectral Element Method (SEM). This method uses the dynamic stiffness matrix for a periodic model, which is then transformed into a Transfer Matrix (MT). In TM, the Floquet-Bloch Theorem is applied to solve the formed eigenvalue problem. In it, the eigenvalues produce the wavenumber and the eigenvectors to the wave modes, Pereira and Santos [6].

Much work has been done on wave propagation in periodic structures. Orris [7] employed numerical techniques in the analysis of wave propagation. For this, it applied the displacement analysis method , where the study structure is divided into an arbitrary number of discrete elements (nodes). Faulkner [8] applied numerical methods on mono-coupled periodic structures with regularly spaced supports. Thus, it concluded that vibration problems in mono-coupled systems can be analyzed by the combination of finite elements and the transfer matrix. Thus,

it obtained close analytical and computational results. Wu et al. [9] investigated through SEM the properties of bandgaps of a new type of lattice structure with second-order hierarchical periodicity, based on the hierarchical structures of the surface of a butterfly's wing. Pereira [6] analyzed, using the spectral element method, a periodic structure of a closed circular cylindrical shell in two situations: fluid filled and *in vacuum*. This structure was composed of unit cells, where there was a variation in the material that made them up. This proposed structure aims to reduce the effect of vibrations on the elements, also providing noise control.

Han et al. [10] presented a variation of the transfer matrix (MT), defining the modified transfer matrix (MTM). In a one-dimensional PC Euler-Bernoulli beam, it was found that MTM for the calculation of beam vibration has a lower computational cost compared to MT. Edson [11] investigated the effect of attenuation as a function of polyethylene concentration in an Euler-Bernoulli beam. Albino [12] studied the vibrations caused by passing passenger trains, using the 3D Finite Element Method (FEM). PCs were simulated buried and periodically placed between the train line and the passengers, in order to mitigate the effect of vibrations. In this work, therefore, the effect of varying the frequency of vibration in a periodic structure of the rodtype will be analyzed, characterized by the variation of the material and cross section area of the unit cell. The boundary conditions imposed on the model were an excitation at a free end of the rod, while the other end was clamped.

2 SEM analysis in phononic crystal rods.

SEM was applied in a phononic crystal homogeneous rod, with a circular cross section area, as shown in Figure 1. Through SEM in 1D PC structures, it is found a analytic solution using the Transfer Matrix of a unit cell, and then expanding the dynamic analysis to all cells.

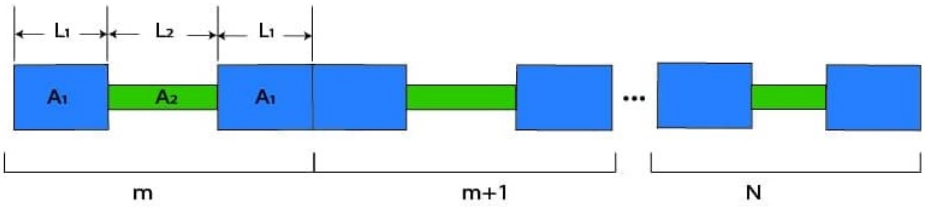

Figure 1. Phononic crystal rod model

According to Lee [13], starting from the free longitudinal vibration of a uniform rod, the relationship between the forces and the nodal displacements are defined by:

$$\boldsymbol{S_R}(\omega)\boldsymbol{d} = \boldsymbol{f}_c(\omega) \tag{1}$$

Where $\boldsymbol{d}$ and $\boldsymbol{f}_c(\omega)$ are the displacements and nodal forces, respectively. $\boldsymbol{S_R}(\omega)$ is the spectral matrix of the finite rod, defined by:

$$\boldsymbol{S_R}(\omega) = \frac{EA}{L}\begin{bmatrix} S_{R11} & S_{R12} \\ S_{R12} & S_{R22} \end{bmatrix} \tag{2}$$

Wherein E is the Young's modulus, A the cross section area, and L the length. $S_{R11} = S_{R22} = (K_L L)\cot(K_L L)$ and $S_{R12} = -(K_L L)\csc(K_L L)$. Wavenumber is defined as a function of frequency (ω) and of the specific (ρ), $k_L = \omega\sqrt{\rho/E}$.

From Equation 2 for a cell from a 1D periodic structure, we obtain the forces and displacements left (L) and right (R) nodes:

$$\begin{Bmatrix} -\boldsymbol{f}_L \\ \boldsymbol{f}_R \end{Bmatrix}_k = \begin{bmatrix} \boldsymbol{S}_{LL}(\omega) & \boldsymbol{S}_{LR}(\omega) \\ \boldsymbol{S}_{RL}(\omega) & \boldsymbol{S}_{RR}(\omega) \end{bmatrix}_k \begin{bmatrix} \boldsymbol{d}_L \\ \boldsymbol{d}_R \end{bmatrix}_k \tag{3}$$

Rearranging the terms of the Equation 3

$$\begin{Bmatrix} \boldsymbol{d}_R \\ \boldsymbol{f}_R \end{Bmatrix}_k = \begin{bmatrix} -\boldsymbol{S}_{LR}^{-1}\boldsymbol{S}_{LL} & -\boldsymbol{S}_{LR}^{-1} \\ \boldsymbol{S}_{RL} - \boldsymbol{S}_{RR}\boldsymbol{S}_{LR}^{-1}\boldsymbol{S}_{LL} & -\boldsymbol{S}_{RR}\boldsymbol{S}_{LR}^{-1} \end{bmatrix}_k \begin{Bmatrix} \boldsymbol{d}_L \\ \boldsymbol{f}_L \end{Bmatrix}_k \tag{4}$$

Renaming the terms of Equation 4

$$\boldsymbol{p}_{kR} = \boldsymbol{T}_{k(\omega)}\boldsymbol{p}_{kL} \tag{5}$$

Where $\boldsymbol{T}_k(\omega)$ is the transfer matrix derived from the spectral element model for the kth cell of the structural network. It is related to vectors $\boldsymbol{p}_{kR}$ and $\boldsymbol{p}_{kL}$. These represent, respectively, the degrees of freedom and forces in the cross section of the cell.

In a 1D Phononic Crystal structure divided into N cells, each cell (m) has the right (R) boundary conditions equal to the boundary conditions of the subsequent cell $(m-1)$, i.e, from the left (L), so that:

$$\begin{aligned} \boldsymbol{d_L}^{(m)} &= \boldsymbol{d_R}^{(m-1)} \\ \boldsymbol{f_L}^{(m)} &= -\boldsymbol{f_R}^{(m-1)} \end{aligned} \tag{6}$$

For an infinite number of unit cells, we can apply the Floquet-Bloch Theorem to obtain:

$$\begin{aligned} \boldsymbol{d_L}^{(m)} &= e^{\psi} \cdot \boldsymbol{d_R}^{(m-1)} \\ \boldsymbol{f_L}^{(m)} &= -e^{\psi} \cdot \boldsymbol{f_R}^{(m-1)} \end{aligned} \tag{7}$$

Where, $\psi = ik_bL_c$ is called the Bloch parameter [14], i is the imaginary number, k_b the Bloch wavenumber, and L_c the length of the unit cell. Replacing Equation 7 in Equation 5,there is the eigenvalue problem:

$$\boldsymbol{p}\boldsymbol{T}_{\boldsymbol{k(\omega)}} = e^{\psi}\boldsymbol{p} \tag{8}$$

The e^{ψ} is the eigenvalue, which produces the Bloch wavenumber (k_b), which corresponds to the wave propagation modes in the structure.

3 Numerical results

Using the rod model represented in Figure 2, the rod boundary conditions are Clamped-Free with an excitation at the free end. The forced responses were obtained by applying the transfer matrix (MT) method to a cell, and then raising the result to the total number of cells.

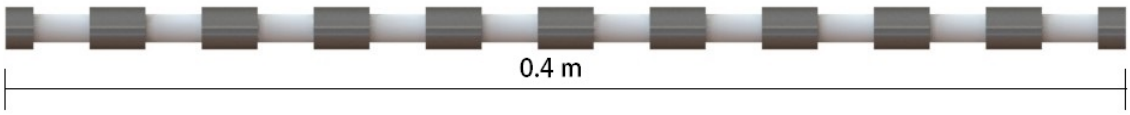

Figure 2. Phononic crystal rod

Figure 2 represents the used rod model, which is divided into 10 equal Cells, in which each cell is composed of Steel and Polyacetal, being divided into three parts. The end parts are made of Steel, while the central part is made of Polyacetal. Figure 3 represents the unit cells with the same cross section area for a given material proportion. The geometric and material properties are shown in Table 1.

3.1 Bandgaps and Attenuation Regions

The characteristic regions of PCs can be seen in Figure 4. In which Figure 4a and 4c represent the Frequency Response Function (FRF) of the Receptance and Figure 4b and 4d represent the regions of bandgaps, for cells shown in Figure 3. The shaded areas represent the first attenuation region. The solid blue lines represent the

(a) (b)

Figure 3. a) cell composed of 90% Steel and 10% Polyacetal b) cell composed of 50% Steel and 50% Polyacetal

Table 1. Geometric and material properties of the rod

Geometry and material	Nomenclature	Value/formulation
Number of cell	N	10
Rod length	L	0.4 $[m]$
Cell length	L_{cell}	0.04 $[m]$
Filling constant	α	10% - 80%
Area constant	β	0% - 50%
Cell's Steel filling	L_1	$\alpha \cdot L_{cell}/2$ $[m]$
Cell's Polyacetal filling	L_2	$L_{cell} \cdot (1-\alpha)$ $[m]$
Polyacetal's circular cross-section area	A_1	0.0079 $[m^2]$
Steel's circular cross-section area	A_2	$(\beta+1) \cdot A_1$ $[m^2]$
Young's modulus (Steel and Polyacetal)	E_s, E_p	$210 \cdot 10^9$and $2.41 \cdot 10^9$ $[Pa]$
Mass density (Steel and Polyacetal)	ρ_s, ρ_p	7860 and 1140 $[kg/m^3]$
Damping factor	η	0.01
Poisson's ratio (Steel and Polyacetal)	ν	0.30 and 0.35

SEM method, while the dashed red lines represent the FEM with 300 elements. The results between the analytical method (SEM) and the approximation method (FEM), converging to each other. Figures 4b and 4d shows the dispersion curves and refers to Bloch's wavenumber. The cell corresponding to Figures 4a and 4b has a proportion of $\alpha = 0,9$, i.e, 10% of Polyacetal and 90% of Steel, while the cell corresponding to Figures 4c and 4d has a 50-50% proportion of Polyacetal and Steel ($\alpha = 0,5$). It is possible to verify the attenuation and bandgap regions in certain frequency bands, as in Figure 4a, which has two large bandgap regions, the first bandgap band between the 13KHz and 70KHz regions (shaded area) and the second between 72KHz and 140KHz KHz, which can be identified with the imaginary part of the Bloch wavenumber different from zero, and therefore, in the same frequency range in the graph of Figure 4b, there is an attenuation region, which corresponds to the region that has the propagation of totally evanescent waves, which makes this region free of oscillation. In Figure 4d, with the increase in the concentration of Polyacetal in the cell, there are several regions of bandgaps, which results in an increase in the passing band regions, in which there are propagating waves, and a decrease in the attenuation regions, which can be verified comparing Figures 4a and 4c.

3.2 Parametric area variation

The value of the end-cell area in Figure 1 was varied according to β (0% - 50%) more than the value of the central-cell area, while the material concentrations were fixed at α. The values of α at each stage were varied from 10% until 80%.

The imaginary part of the Bloch number is represented by $\Im(kL) = f(\rho, E_c, A, L, \omega, K)$, on what E_c represents the complex elastic modulus, varying only the area and frequency, its sensitivity can be related to powered by $\Im(kL) = f(\omega, A)$. Figure 5a represents the 3D graph of $\Im(kL)$ for a concentration of 20% Polyacetal and 80% Steel, while Figure 5b represents the receptance graph of the same cell.

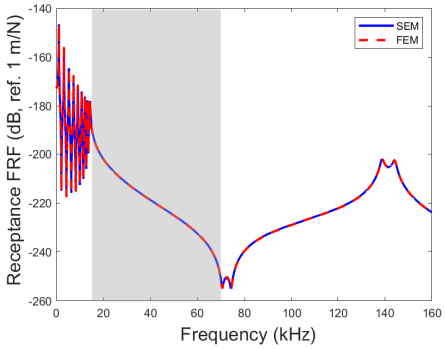

(a) FRF receptance for a cell composed of 90% Steel and 10% Polyacetal

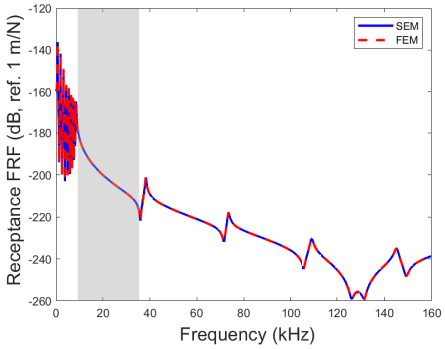

(c) FRF receptance for a cell composed of 50% Steel and 50% Polyacetal

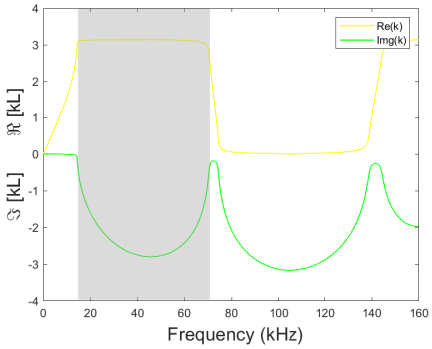

(b) Bloch wavenumber for a cell composed of 90% Steel and 10% Polyacetal

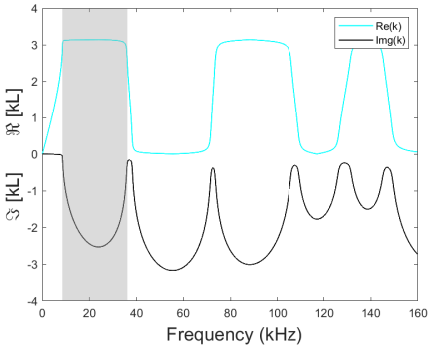

(d) Bloch wavenumber for a cell composed of 50% Steel and 50% Polyacetal

Figure 4. FRF receptance of a rod with 10 unit cells (a and c). Dispertion curves of a cell (b and d).

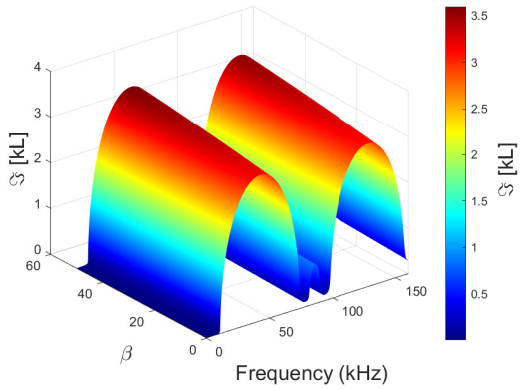

(a) Parametric analysis of a cell with $\alpha = 0.8$ and ranging β.

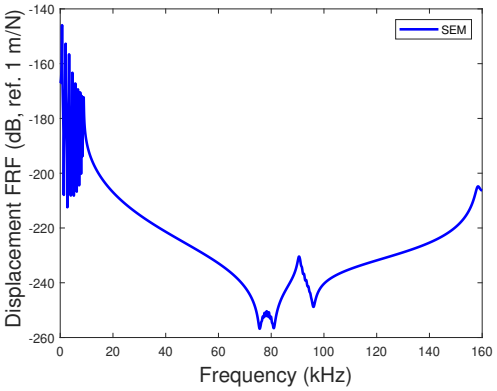

(b) Frequency response function of displacement for the most intense atenuation.

Figure 5. Parametric analysis of the wavenumber.

Figure 6 represents a parametric analysis of one cell. The parameters varied to form the dispersion curves ($Im(kL)$) were the frequency, cross section area (β) and material proportion in each cell (α). It is possible to observe that with the increase of β, in all configurations there was an increase in the attenuation intensity, caused by the increase in cell impedance. Figure 6a represents 90% Polyacetal and 10% Steel in one cell . It is observed that, regardless of the value of β, large attenuation values are not observed in regions up to 40 KHz. With the increase of the Steel concentration in the cell, the passing band appears, and consequently the change in the attenuation areas, in all configurations it is verified that with the increase of the edge area, the attenuation intensity also becomes greater. Figure 6h represents the greatest attenuation and destructive effect of Bragg, in the bands of 20-70 KHz and 110-150 KHz.

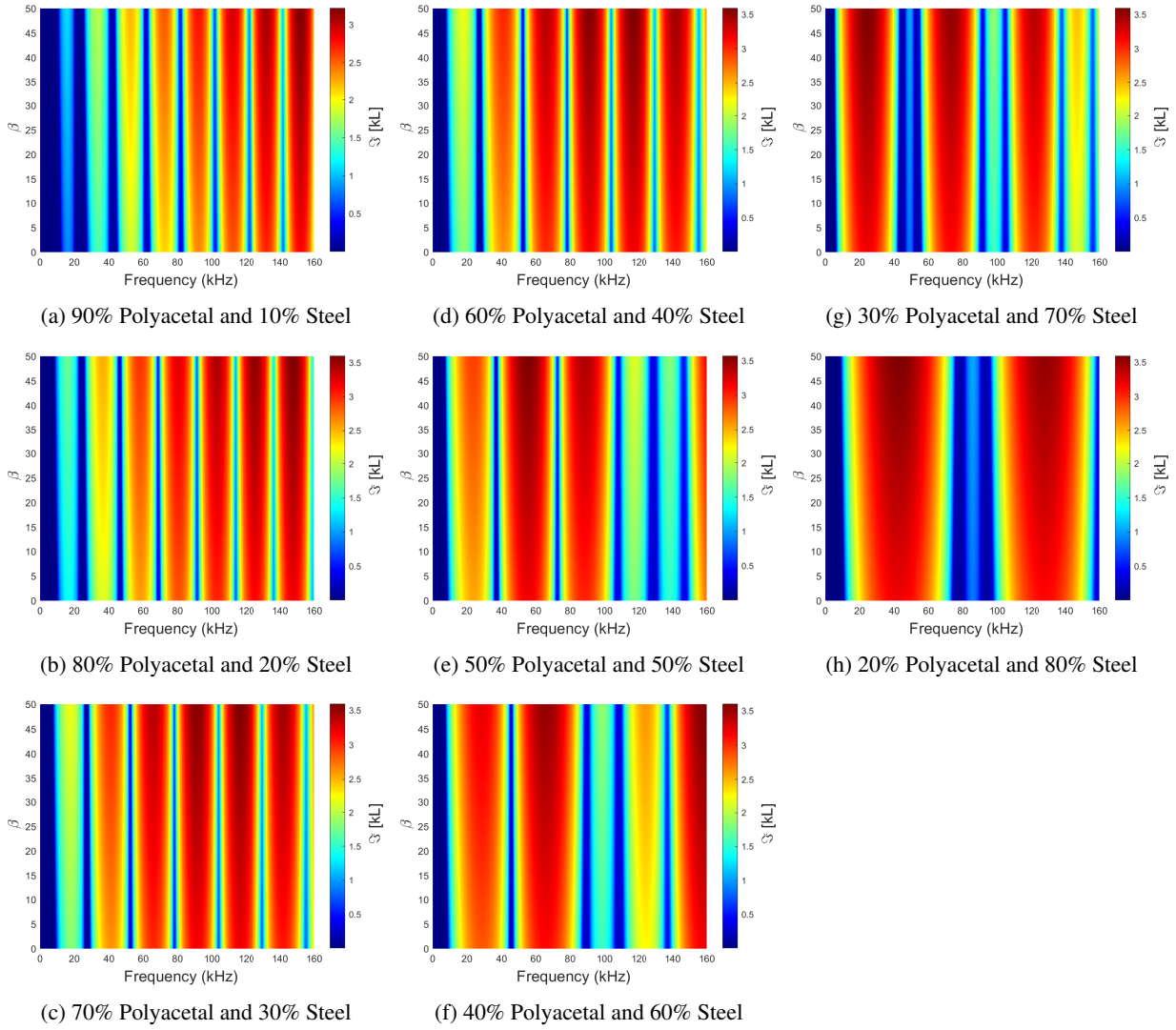

(a) 90% Polyacetal and 10% Steel

(b) 80% Polyacetal and 20% Steel

(c) 70% Polyacetal and 30% Steel

(d) 60% Polyacetal and 40% Steel

(e) 50% Polyacetal and 50% Steel

(f) 40% Polyacetal and 60% Steel

(g) 30% Polyacetal and 70% Steel

(h) 20% Polyacetal and 80% Steel

Figure 6. Imaginary part of wavenumber, varying as a function of frequency and cross section. For each subfigure, there is a cross section variation for a fixed proportion of material (α).

Figure 6g acquires a configuration of higher intensities with frequencies in the range of 15-50 KHz and 130-160 KHz, while it has lower attenuations in the central bands, between 60-120 KHz. Figure 6f has a region between 90-110 KHz of low attenuation. For Figures 6a and 6b it occurs that regions with high attenuation are formed at higher frequency, in addition to having a region of low attenuation up to 30 KHz, while for 6e and 6f regions with higher frequencies have low attenuation.

It was also possible to observe the coupling of the effects in the Bragg's scattering due to changes in the cross section area and proportion of material. This changes caused an increase in both attenuation intensity and frequency range where attenuation occurred.

4 Conclusions

This article presents the wave propagation in a 1D Phononic Crystal rod, in which the FRF and the Bloch wavenumber were obtained. The validation of the results was made comparing the values obtained in the SEM and FEM methods, obtaining agreement between the results. With the increase in the difference between the areas of Steel and Polyacetal materials, there was an increase in the attenuation value, due to the increase in impedance in the cell.

The variation of area and material in a fixed unit cell of the phononic crystal was also used. The change in the concentration of Polyacetal and Steel in the rod has an effect on the cell attenuation. Even more, in some regions there is no wave propagation, regardless of the concentration of material in the cell or variation of the peripheral

area. Frequency regions where the attenuation effect in a cell characteristic did not occur may start to appear. This was caused by the coupling effect of the Bragg scattering.

Acknowledgements. The authors thank the Graduate Program in Mechanical Engineering (UFMA)
Authorship statement. The authors hereby confirm that they are the sole liable persons responsible for the authorship of this work, and that all material that has been herein included as part of the present paper is either the property (and authorship) of the authors, or has the permission of the owners to be included here.

References

[1] R. B. Santos. An alternative approach to design periodic rods. *Doctoral thesis - Faculdade de Engenharia, Universidade Estadual Paulista, Ilha Solteira, SP*, 2018.
[2] D. Mead. Free wave propagation in periodically supported, infinite beams. *Journal of Sound and Vibration*, vol. 11, n. 2, pp. 181–197, 1970.
[3] M. S. Kushwaha, P. Halevi, L. Dobrzynski, and B. Djafari-Rouhani. Acoustic band structure of periodic elastic composites. *Phys. Rev. Lett.*, vol. 71, pp. 2022–2025, 1993.
[4] M. Sigalas and E. N. Economou. Elastic and acoustic wave band structure. *Journal of Sound and Vibration*, vol. 158, pp. 377–382, 1992.
[5] M. I. Hussein, M. J. Leamy, and M. Ruzzene. *Dynamics of Phononic Materials and Structures: Historical Origins, Recent Progress, and Future Outlook*, volume 66. ASME International, 2014.
[6] F. Pereira and J. D. Santos. *Phononic crystal investigation using a fluid-structure circular cylindrical shell spectral element*, volume 148. Elsevier BV, 2020.
[7] R. M. Orris and M. Petyt. *A finite element study of harmonic wave propagation in periodic structures*, volume 33. Elsevier BV, 1974.
[8] M. Faulkner and D. Hong. *Free vibrations of a mono-coupled periodic system*, volume 99. Elsevier BV, 1985.
[9] Z. Wu, F. Li, and C. Zhang. *Band-gap analysis of a novel lattice with a hierarchical periodicity using the spectral element method*, volume 421. Elsevier BV, 2018.
[10] L. Han, Y. Zhang, Z.-Q. Ni, Z.-M. Zhang, and L.-H. Jiang. *A modified transfer matrix method for the study of the bending vibration band structure in phononic crystal Euler beams*, volume 407. Elsevier BV, 2012.
[11] de E. J. P. Miranda Jr and J. M. C. D. Santos. *Flexural wave band gaps in phononic crystal Euler-Bernoulli beams using wave finite element and plane wave expansion methods*, 2017.
[12] C. Albino, L. Godinho, P. Amado-Mendes, P. Alves-Costa, da D. D. Costa, and D. Soares. *3D FEM analysis of the effect of buried phononic crystal barriers on vibration mitigation*, volume 196. Elsevier BV, 2019.
[13] U. Lee. *Spectral Element Method in Structural Dynamics*. John Wiley & Sons, 2009.
[14] A. Hvatov and S. Sorokin. Free vibrations of finite periodic structures in pass- and stop-bands of the counterpart infinite waveguides. *Journal of Sound and Vibration*, vol. 347, pp. 200–217, 2015.